Electronic Supplementary Material (ESI) for ChemComm.

Supporting Information

Novel mode of 2-fold interpenetration observed in a primitive cubic network of formula [Ni(1,2-bis(4-pyridyl)acetylene)(Cr_2O_7)]$_n$

Hayley S. Scott,† Alankriti Bajpai,† Kai-Jie Chen,† Tony Pham,‡ Brian Space,‡ John. J. Perry IV,† and Michael J. Zaworotko*,†

†Department of Chemical and Environmental Science, Materials and Surface Science Institute, University of Limerick, Co. Limerick, Ireland

‡Department of Chemistry, CHE205, University of South Florida, 4202 East Fowler Avenue, Tampa, Florida 33620, United States

Experimental

General

All reagents and solvents were purchased from Sigma-Aldrich and used as received.

Fourier Transform Infrared spectra were measured on a Perkin Elmer Spectrum 100 spectrometer with Universal ATR accessory between the range of 4000-650 cm^{-1}.

Powder X-ray diffraction analyses were performed with a Philips X'Pert PRO MPD, equipped with a Cu-*K*α source. Patterns were collected from 4° to 40° 2θ, using a step size of 0.02° at a scan rate of 0.1°min^{-1}.

Thermogravametric analyses were performed on a TA Instruments Q50 TG from ambient temperature to 500° C, at a scan rate of 10° min^{-1}, under a flow of N_2.

Gas sorption isotherms were measured using Micromeritics Tristar II 3030 and 3Flex 3500 surface characterisation analysers.

X-ray crystallographic measurements were collected at 100(2) K on a Bruker Quest D8 Cu Microfocus with Cu-Kα radiation (λ = 1.5418 Å). The data collection and integration were performed within SMART and SAINT+ software programs,[1] and corrected for absorption using the multi-scan method implemented in SADABS.[2]

Crystallographic data and refinement parameters for **DICRO-2-Ni-i**, given in Table S1, were solved by direct methods (SHELXS-97), and refined (SHELXL-97) by full least-squares on all F^2 data.[3] All other non-hydrogen atoms were refined anisotropically and all hydrogen atoms were placed in calculated positions.

Single crystals of **DICRO-2-Ni-i** were very small and weakly diffracting. Consequently, a number of restraints have been placed on atoms and level alerts A and B appear in the Checkcif. The contribution of the disordered solvent molecules was subtracted from the reflection data by the SQUEEZE method as implanted in the program PLATON.[3b]

DICRO-2-Ni-i was refined as a racemic twin, using SHELX-97,[3] and a BASF refined to 0.52452 was obtained. The RIGU restraint has been placed on selected atoms. The pyridyl ring incorporating atoms N1C1C2C3C4C5 has been modelled over two positions using a free variable.

Synthesis

4,4'-(1,2-ethynediyl)bis-pyridine was made following a previously published method.[4]

Single crystals:

$NiCl_2 \cdot 6H_2O$ (23 mg, 0.1 mmol) and $K_2Cr_2O_7$ (29 mg, 0.1 mmol) were dissolved in 3 ml H_2O and the aqueous solution pipetted into a long, thin test-tube. Carefully layered on top of that was a 5 ml solution of H_2O:MeCN (1:1, v:v). A solution of 4,4'-(1,2-ethynediyl)bis-pyridine (**2**) (18 mg, 0.1 mmol) dissolved in 3 ml MeCN was then layered on top of this and the test-tube sealed and left to stand. After two weeks, very small yellow block shaped crystal had formed.

Mw 635.09; Yield ~10 mg (15 %); IR (ATR, cm^{-1}) 2951 (w), 1605 (s), 1548 (m), 1505 (s), 1420 (s), 1323 (w), 1212 (s), 1061 (s), 1020 (s), 929 (s), 882 (w), 870 (s), 824 (s), 768 (s), 729 (s), 667 (s).

Initially, single crystals were formed via diffusion reactions, as above. However, due to low yield a scaled up, bulk powder synthesis method was employed. Additionally, bulk powder syntheses were adapted to suit the stoichiometry of the single crystal product.

Powdered sample:

$NiCl_2 \cdot 6H_2O$ (65 mg, 0.27 mmol) and $K_2Cr_2O_7$ (81 mg, 0.27 mmol) were dissolved in 6 ml H_2O and stirred. Separately, 4,4'-(1,2-ethynediyl)bis-pyridine (**2**) (100 mg, 0.55 mmol) was dissolved in 20 ml MeCN and added drop wise to the stirring aqueous solution. A yellow precipitate formed immediately. The solution was left stirring for 18 hrs, after which time the precipitate was filtered and washed with 5 ml H_2O, followed by 5 ml MeCN.

Mw 635.09; Yield 124 mg (72 %); IR (ATR, cm^{-1}) 3065 (w), 1610 (s), 1547 (s), 1505 (s), 1421 (s), 1213 (s), 1062 (s), 1020 (s), 954 (s), 931 (s), 883 (w), 870 (s), 827 (s), 769 (s), 730 (s), 668 (s).

Activation:

After filtration, the product was dispersed in 8 ml MeCN and the solvent exchanged once a day for three weeks. Following this, the product was filtered and washed with a further 10 ml of MeCN. To activate the sample, the compound was placed under reduced pressure (0.0030 mmHg) at ambient temperature for 16 hrs.

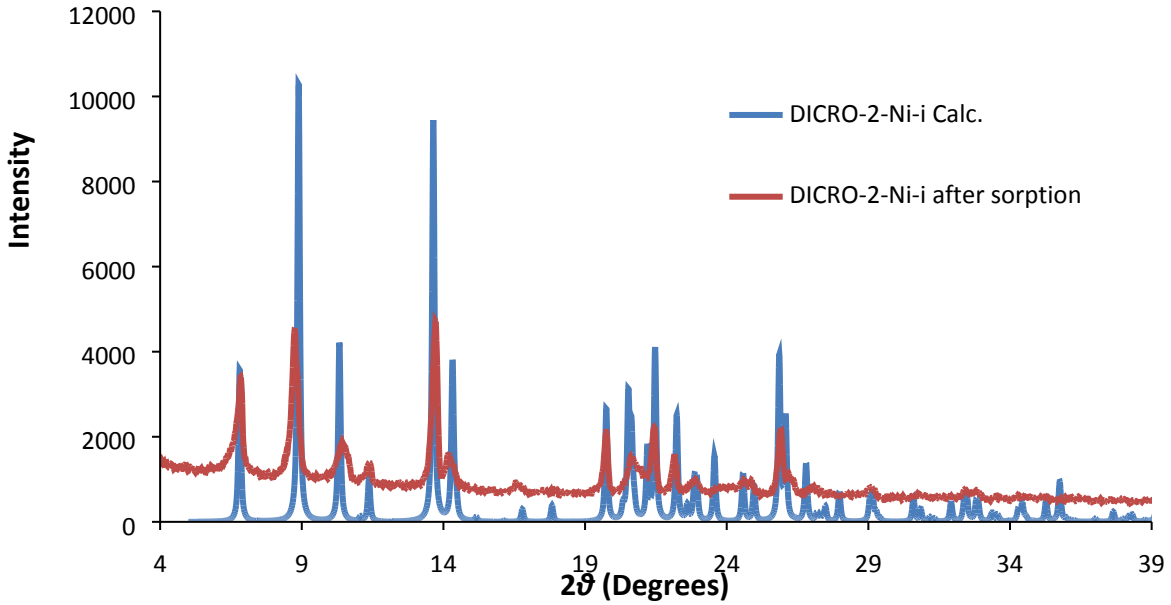

Figure S1. Post-activation experimental and calculated powder X-ray diffraction patterns for **DICRO-2-Ni-i**.

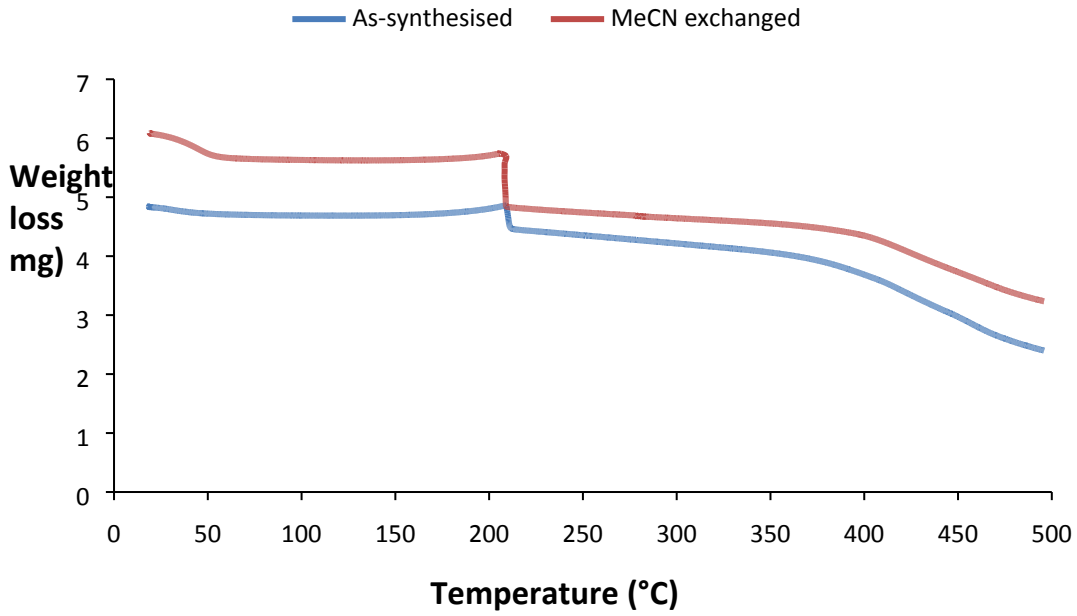

Figure S2. Thermogravimetric analysis of **DICRO-2-Ni-i** between 20-500 ˚C, at a scan rate of 10 ˚C/min.

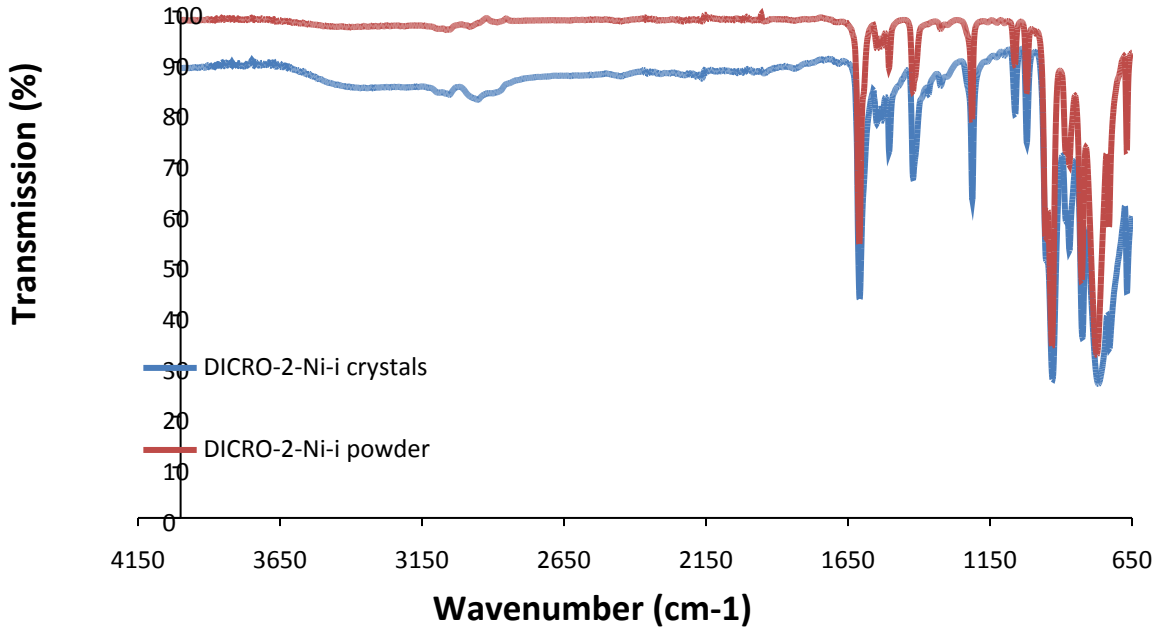

Figure S3. Infrared spectrum of crystals and powdered samples of **DICRO-2-Ni-i**.

Crystallographic Data

Table S1. Crystal data and refinement details.

Compound	**DICRO-2-Ni-i**
Formula	$C_{24}H_{16}Cr_2N_4Ni_1O_7$
Mw (g mol^{-1})	635.12
T (K)	100
Crystal system	Orthorhombic
Space group	*I*222
Z	4
a (Å)	8.5465(9)
b (Å)	15.9683(17)
c (Å)	20.726(2)
β (°)	90
V (Å^3)	2828.6(5)
ρ_{calc} (g cm^{-3})	1.491
μ (mm^{-1})	7.403
Measured/independent Reflections (R_{int})	4201/1489(0.1475)
Observed reflections [I > 2σ(I)]	719
R_1[a], wR_2[b] [I > 2σ(I)]	0.0956, 0.2040
R_1, wR_2 (all data)	0.1902, 0.2406
Goodness-of-fit on F^2	1.014

[a] $R_1 = \sum||F_o| - |F_c||/\sum|F_o|$. [b] $wR_2 = \{\sum[w(F_o^2\sum F_c^2)^2]/\sum[w(F_o^2)]\}^{1/2}$

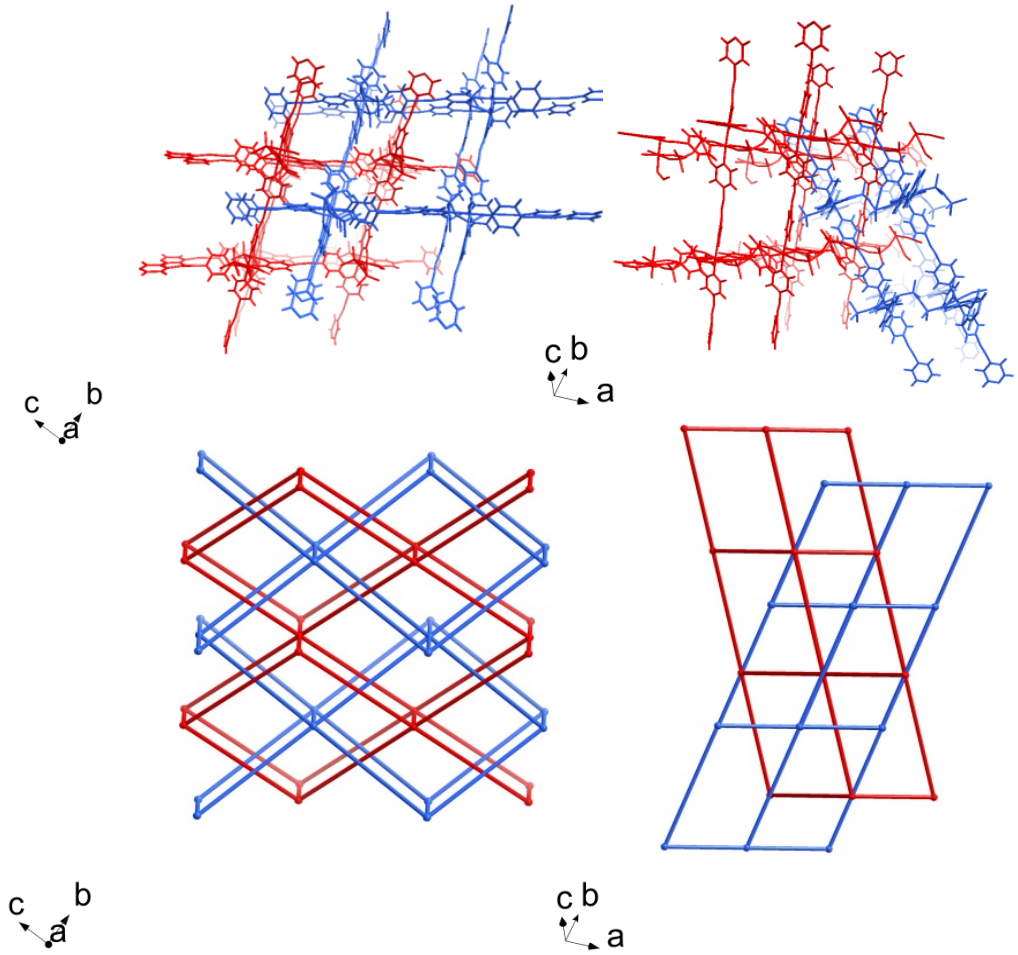

Figure S4. (Top left) **DICRO-2-Ni-i**, with the two

interpenetrating frameworks in red and blue. Frameworks interpenetrated in a diagonal/diagonal inclined arrangement, (Top right) Structure rotated 90°, highlighting inclined arrangement of entanglement. (Bottom) Corresponding topological representations of the two networks.

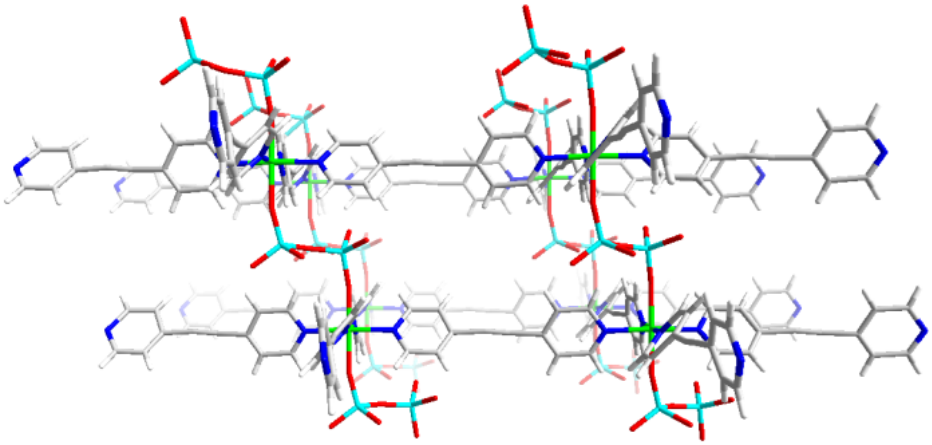

Figure S5. Single framework of **DICRO-2-Ni-i** orientated to show the angular or "stepped" arrangement of dichromate pillars in **DICRO-2-Ni-i**.

Calculation of isosteric heat of adsorption

The *Q*st value for **DICRO-2-Ni-i** was calculated according to the virial equation using the fitted adsorption isotherms at three temperatures (273, 283 and 298 K)

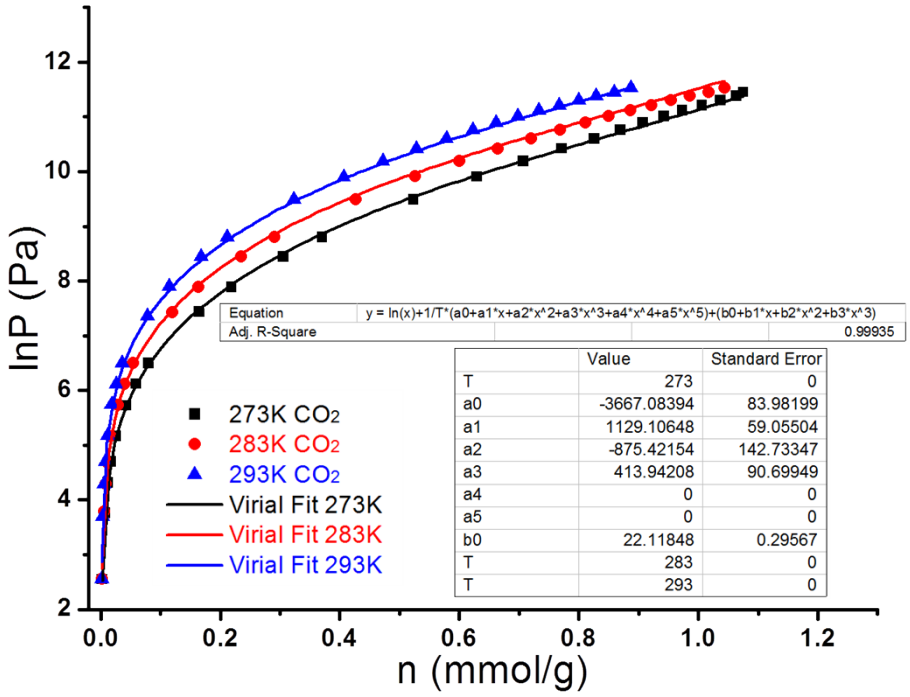

Figure S6. CO_2 adsorption isotherms of **DICRO-2-Ni-i** at 273 K, 283 K and 298 K fitted using the virial equation.

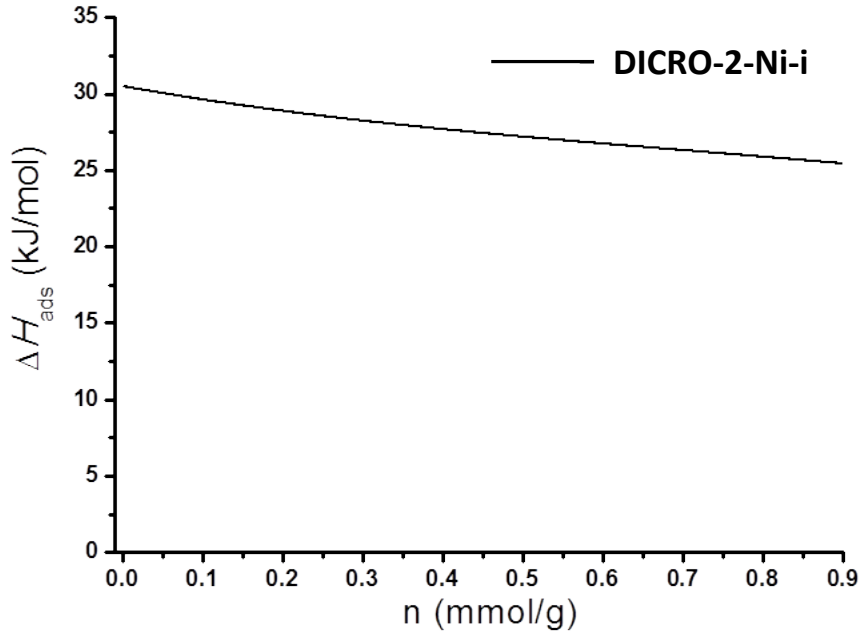

Figure S7. CO_2 isosteric heats of adsorption (Qst) of **DICRO-2-Ni-i** using the fitted data measured at three temperatures (273 K, 283 K and 273 K).

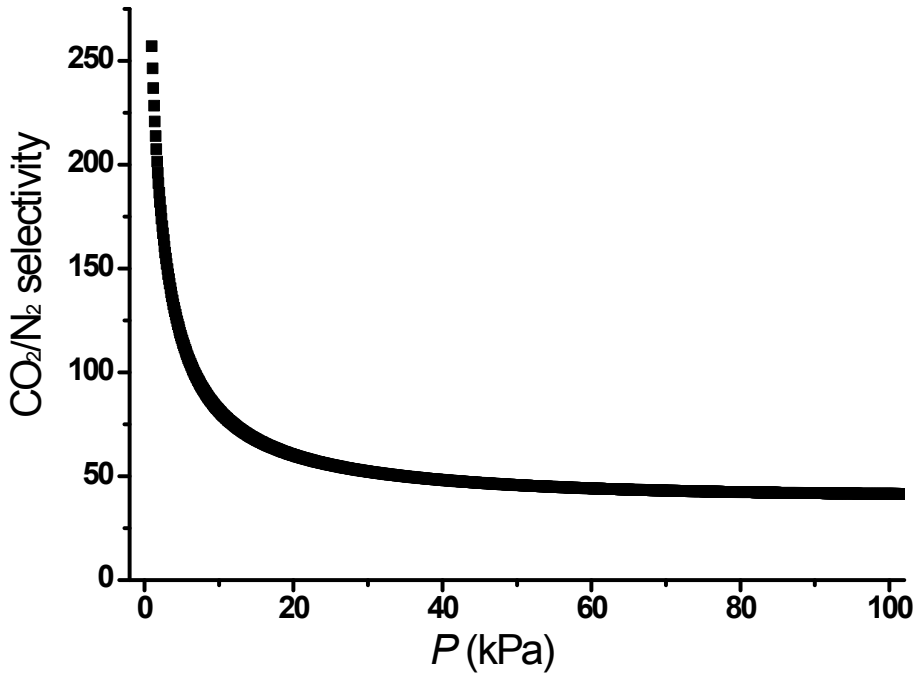

Figure S8. The IAST selectivity of CO_2/N_2 (15% CO_2 and 85% N_2) as function of pressure.

Modeling Details

Simulations of CO_2 adsorption were performed in **DICRO-2-Ni-i** using grand canonical Monte Carlo (GCMC) methods[5] in a 3 × 2 × 1 system cell of the MOM. A spherical cut-off distance of 10.363 Å was used for the simulations; this value corresponds to half the shortest system cell dimension length. A five-site polarizable potential that was developed previously for CO_2 was used for the simulations in this work.[6] The total potential energy of the MOM–CO_2 system was calculated through the sum of the repulsion/dispersion, electrostatic, and polarization energies. These were calculated using the Lennard-Jones potential, partial charges with Ewald summation,[7] and a Thole-Applequist type model,[8] respectively. The chemical potential for CO_2 was determined for a range of temperatures through the Peng-Robinson equation of state.[9] All simulations were performed using the Massively Parallel Monte Carlo (MPMC) code.[10] For all state points considered, the simulations consisted of 5 × 10^6 Monte Carlo steps to guarantee equilibration, followed by an additional 5 × 10^6 steps to sample the desired thermodynamic properties.

The parametrization of **DICRO-2-Ni-i** was performed as follows. The Lennard-Jones parameters (ε and σ) for all aromatic C, H, and N atoms were taken from the Optimized Potentials For Liquid Simulations – All Atom (OPLS-AA) force field,[11] while such parameters for Ni, Cr, and O were taken from the Universal Force Field (UFF).[12] The partial charges for the chemically distinct atoms in **DICRO-2-Ni-i** (Figure S7) were determined through periodic fitting of the entire crystal structure using the Vienna *ab initio* Simulation Package (VASP)[13] with the projector augmented wave (PAW) method[14] and Ceperley–Alder (CA) functional.[15]A restraining potential was implemented to treat the presence of buried atoms in the structure. The calculations were performed using a charge fitting code that was developed previously.[16,17] The final partial charges for each chemically distinct atom in **DICRO-2-Ni-i** can be found in Table S2.

The exponential damping-type atomic point polarizabilities for all C, H, N, and O atoms were taken from a carefully parametrized set provided by the work of van Duijnen and Swart.[18] The polarizability parameters for Ni^{2+} and Cr^{6+} were determined by fitting a molecular polarizability tensor to one that was obtained from quantum mechanical calculations for fragments containing Ni^{2+} and Cr^{6+}, respectively, according to previous considerations.[19] These calculations were performed using the Q-Chem code[20] with the aug-cc-pVDZ basis set applied to all atoms. An average value of 2.94650 $Å^3$ and 3.50740 $Å^3$ was calculated for Ni^{2+} and Cr^{6+}, respectively. These polarizability values were assigned to the nuclear centers of all atoms of the framework to model explicit polarization.

The simulated CO_2 adsorption isotherms in **DICRO-2-Ni-i** at 273, 283, and 293 K are compared with the matching experimental data in Figure S8. The calculated CO_2 uptakes at the various temperatures are in good agreement with the corresponding experimental isotherms. Consistent with experimental measurements, the simulated CO_2 uptakes in **DICRO-2-Ni-i** are quite low within the pressure range considered (0–1 atm), thus suggesting that there is little room for the CO_2 molecules to occupy in this material. Examination of the modeled structure at CO_2 saturation revealed that the CO_2 molecules can only adsorb into the noticeable channel that can be viewed along the *a*-axis in the MOM (Figure S9). The inorganic channels are too narrow to be accessible for adsorbate molecules.

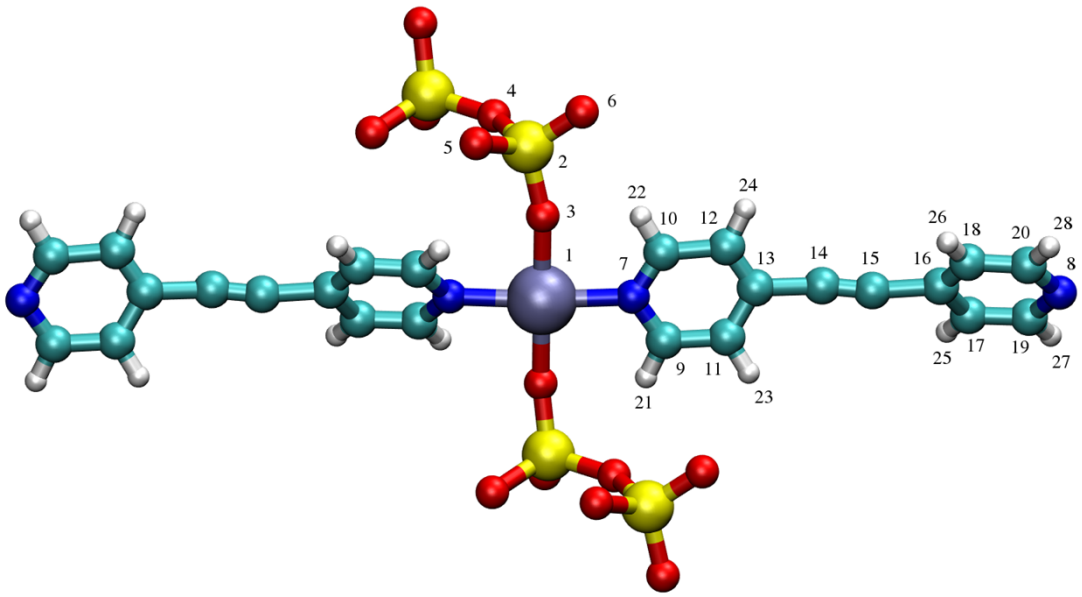

Figure S9: The chemically distinct atoms in **DICRO-2-Ni-i** defining the numbering system corresponding to **Table S2**. Atom colors: C = cyan, H = white, N = blue, O = red, Cr = yellow, Ni = lavender.

Table S2: The partial charges (in e^-) for the chemically distinct atoms in **DICRO-2-Ni-i** Numerical labeling of atoms correspond to **Figure S7**.

Atom	**Label**	***q*** **(e^-)**
Ni	1	0.82300
Cr	2	1.25560
O	3	-0.56430
O	4	-0.50640
O	5	-0.53110
O	6	-0.54910
N	7	-0.14170
N	8	-0.20880
C	9	0.11370
C	10	0.17490
C	11	-0.52930
C	12	-0.36100

C	13	0.35280
C	14	-0.15110
C	15	-0.10070
C	16	0.39970
C	17	-0.37800
C	18	-0.38020
C	19	0.16800
C	20	0.12730
H	21	0.04950
H	22	0.04310
H	23	0.12160
H	24	0.20580
H	25	0.24160
H	26	0.20290
H	27	0.19070
H	28	0.08980

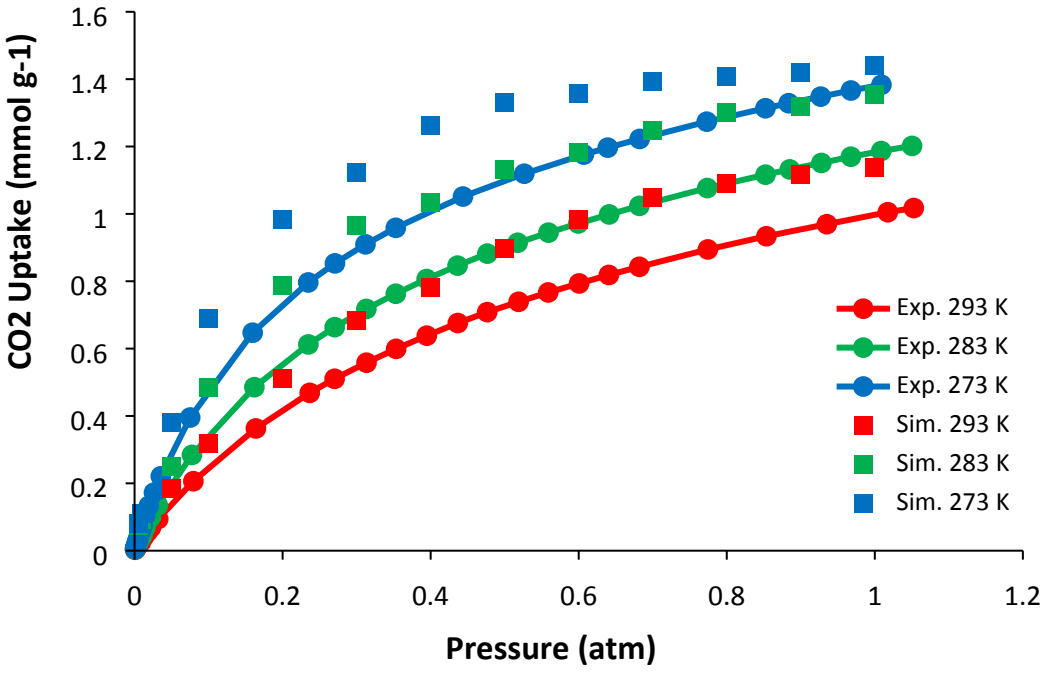

Figure S10: Experimental (lines with circles) and simulated (squares) CO_2 adsorption isotherms in **DICRO-2-Ni-i** at 273 (blue), 283 (green), and 298 K (red).

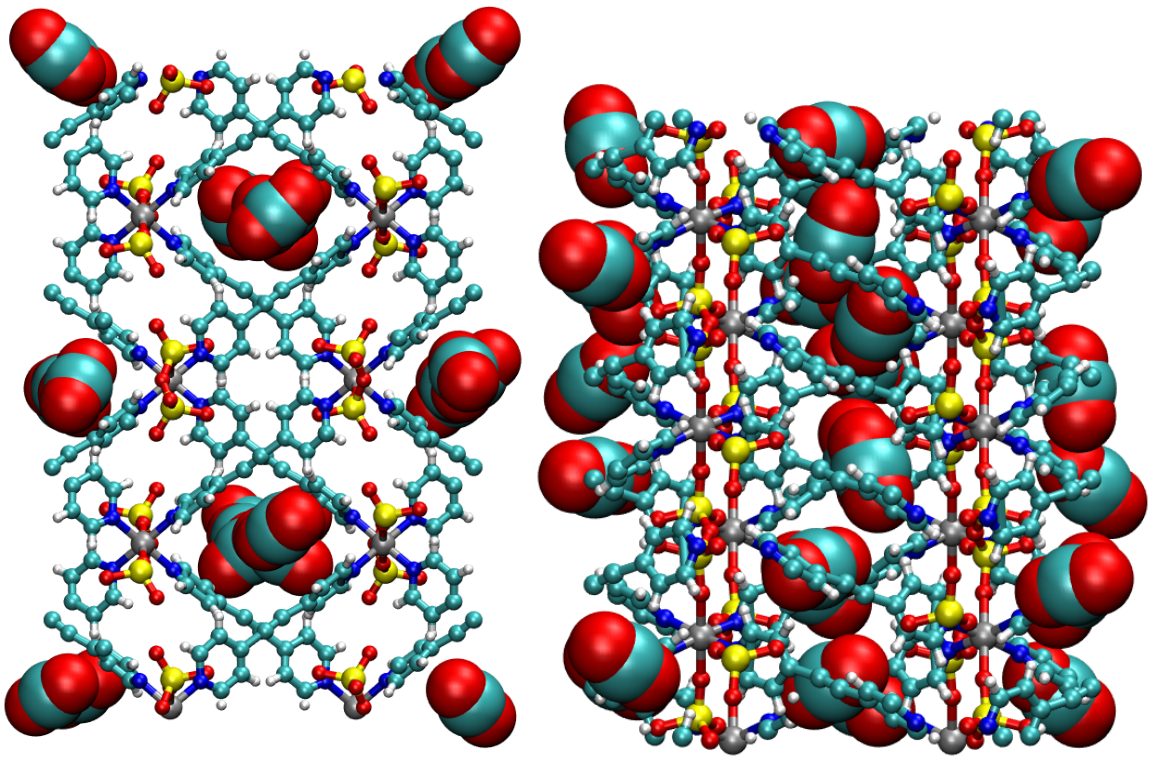

(a) (b)

Figure S11: (a) The *a*-axis view and (b) *b*-axis view of the modeled 3 × 2 × 1 system cell of **DICRO-2-Ni-i** at CO_2 saturation. Atom colors: C = cyan, H = white, N = blue, O = red, Cr = yellow, Ni = silver.

References for Supporting Information:

1. Bruker, SAINT+, Data Reduction Software, Bruker AXS Inc., Madison, Wisconsin, USA

2. G. M. Sheldrick, SADABS, Program for area detector adsorption correction, Institute for Inorganic Chemistry, University of Göttingen, Germany, 1996.
3. (a). G. M. Sheldrick, SHELXL-97, Program for refinement of crystal structures, University of Göttingen, Germany, 1997. (b). A. L. Spek, *Acta Crystallogr., Sect. A,* 1990, **46**, C34.
4. P. Moreno-García, M. Murat Gulcur, D. L. Manrique, T. Pope, W. Hong, V. Kaliginedi, C. Huang, A. S. Batsanov, M. R. Bryce, C. Lambert and T. Wandlowski, *J. Am. Chem. Soc*., 2013, **135**, 12228
5. N. Metropolis, A. W. Rosenbluth, M. N. Rosenbluth, A. H. Teller and E. Teller, *J. Chem. Phys.,* 1953, **21**, 1087.
6. A. L. Mullen, T. Pham, K. A. Forrest, C. R. Cioce, K. McLaughlin and B. Space, *J. Chem. Theory Comput*., 2013, **9**, 5421.
7. P. P. Ewald, *Ann. Phys*., 1921, **369**, 253.
8. (a) J. Applequist, J. R. Carl and K.-K. Fung, *J. Am. Chem. Soc*., 1972, **94**, 2952. (b) B. Thole, *Chem. Phys*., 1981, **59**, 341. (c) K. A. Bode and J. Applequist, *J. Phys. Chem*., 1996, **100**, 17820. (d) K. McLaughlin, C. R. Cioce, T. Pham, J. L. Belof and B. Space, *J. Chem. Phys*., 2013, **139**, 184112.
9. D.-Y. Peng and D. B. Robinson, *Ind. Eng. Chem., Fundam*. 1976, **15**, 59.
10. J. L. Belof and B. Space, *Massively Parallel Monte Carlo (MPMC)*. 2012, Available on GitHub. https://github.com/mpmccode/mpmc.
11. W. L. Jorgensen, D. S. Maxwell and J. Tirado-Rives, *J. Am. Chem. Soc*., 1996, **118**, 11225.
12. A. K. Rappé, C. J. Casewit, K. S. Colwell, W. A. Goddard and W. M. Skiff, *J. Am. Chem. Soc*., 1992, **114**, 10024.
13. (a) G. Kresse and J. Hafner, J. *Phys. Rev. B,* 1993, **47**, 558. (b) G. Kresse and J. Hafner, *J. Phys. Rev. B,* 1994, **49**, 14251. (c) G. Kresse and J. Furthmüller, *Comput. Mater. Sci*., 1996, **6**, 15. (d) G. Kresse and J. Furthmüller, *Phys. Rev. B,* 1996, **54**, 11169.
14. P. E. Blöchl, *Phys. Rev. B* 1994, **50**, 17953.
15. D. M. Ceperley and B. J. Alder, *Phys. Rev. Lett*., 1980, **45**, 566.
16. D.-L. Chen, A. C. Stern, B. Space and J. K. Johnson, *J. Phys. Chem. A,* 2010, **114**, 10225.
17. A. C. Stern, Ph.D. Thesis, University of South Florida, 2010.
18. P. T. van Duijnen and M. Swart, *J. Phys. Chem. A,* 1998, **102**, 2399.
19. (a) A. C. Stern, J. L. Belof, M. Eddaoudi and B. Space, *J. Chem. Phys*., 2012, **136**, 034705. (b) K. A. Forrest, T. Pham, K. McLaughlin, J. L. Belof, A.C. Stern, M. J. Zaworotko and B. Space, *J. Phys. Chem., C* 2012, **116**, 15538. (c) K. A. Forrest, T. Pham, A. Hogan, K. McLaughlin, B. Tudor, P. Nugent, S. D. Burd, A. Mullen, C. R. Cioce, L. Wojtas, M. J. Zaworotko and B. Space, *J. Phys. Chem. C,* 2013, **117**, 17687.
20. Y. Shao, L. F. Molnar, Y. Jung, J. Kussmann, C. Ochsenfeld, S. T. Brown, A. T. B. Gilbert, L. V. Slipchenko, S. V. Levchenko, D. P. O'Neill, R. A. DiStasio Jr, R. C. Lochan, T. Wang, G. J. O. Beran, N. A. Besley, J. M. Herbert, C. Y. Lin, T. V. Voorhis, S. H. Chien, A. Sodt, R. P. Steele, V. A. Rassolov, P. E. Maslen, P. P. Korambath, R. D. Adamson, B. Austin, J. Baker, E. F. C. Byrd, H. Dachsel, R. J. Doerksen, A. Dreuw, B. D. Dunietz, A. D. Dutoi, T. R. Furlani, S. R. Gwaltney, A. Heyden, S. Hirata, C.-P. Hsu, G. Kedziora, R. Z. Khalliulin, P. Klunzinger, A. M. Lee, M. S. Lee, W.-Z. Liang, I. Lotan, N. Nair, B. Peters, E. I. Proynov, P. A. Pieniazek, Y. M. Rhee, J. Ritchie, E. Rosta, C. D. Sherrill, A. C. Simmonett, J. E. Subotnik, H. L. Woodcock III, W. Zhang, A. T. Bell, A. K. Chakraborty, D. M. Chipman, F. J. Keil, A. Warshel, W. J. Hehre, H. F. Schaefer III, J. Kong, A. I. Krylov, P. M. W. Gill and M. Head-Gordon, *Phys. Chem. Chem. Phys*., 2006, **8**, 3172.